The University of Queensland Australia

SMI MISHC Minerals Industry Safety & Health Centre

Multiple Fires in a Mine Drift with Longitudinal Ventilation

Analysis of fire behaviour of performed fire experiments in a model scale mine drift

Rickard Hansen

Minerals Industry Safety & Health Centre The Sustainable Minerals Institute, The University of Queensland, Australia
P +61 7 3346 4066 F +61 7 3346 4067 E mishc@mishc.uq.edu.au www.mishc.uq.edu.au

Table of Contents

Abstract

The fire behaviour involving multiple fires in a mine drift with longitudinal ventilation was analysed. The conditions and fire phenomena occurring were described. The analysis was based upon experimental data from model-scale fire experiments. A fire involving several fuel items may lead to flames tilted horizontally and filling up the entire cross section, leading to earlier ignition, higher fire growth rates, higher fire spread rate and severe fire behaviour. Longer flame lengths will also result due to decreased air entrainment. A correlation for the continuous flame length was proposed. The results of the analysis will help identifying and preventing potentially dangerous fire situations with several large combustible items distributed along a mine drift.

Nomenclature

A is the cross-sectional area of the mine drift [m^2]
c_p is the specific heat [kJ/kg·K]
D is the diameter of the fire [m]
E is the energy [kJ]
H is the mine drift height [m]
H_f is the vertical distance between the fire source centre and the mine drift ceiling [m]
ΔH_c is the heat of combustion [kJ/g]
L is the length scale
L_f is the flame length [m]
L_f^* is the dimensionless flame length
m is the mass [kg]
$\dot{m}_a$ is the mass flow rate of air [kg/s]
$\dot{Q}$ is the heat release rate [kW]
$\dot{Q}^*$ is the dimensionless heat release rate
S is the free distance between combustible items [m]
S_{avg} is the average free distance between a number of combustible items [m]
t is the time [s]
T_a is the ambient temperature [K]
u is the longitudinal velocity [m/s]
V' is the dimensionless ventilation velocity
V^* is the dimensionless longitudinal velocity
w^* is the characteristic plume velocity
ϕ is the ventilation/fuel controlled criterion
φ is the flame angle formed by the straight line between the centre of the fire and the position of the maximum temperature beneath the mine drift ceiling
ρ_a is the density of the ambient air [kg/m^3]

1. Introduction

In a mine drift with combustible items distributed along the drift, one of the greatest risks would be a continuous fire spread from one larger fuel item to numerous adjacent items where the fire spread is fanned by the longitudinal ventilation. This will result in severe fire behaviour and a major risk to the miners and the fire and rescue personnel.

This paper focuses on the phenomena occurring during the continuous fire spread from item to item in a mine drift with longitudinal ventilation. What conditions and phenomena can be expected during such a fire? Knowing what phenomena that may occur, will allow for better fire design and fire safety at potential sites. When investigating the fire phenomena, experimental data from earlier model-scale fire experiments were applied and analysed. The experimental data was obtained from the model-scale experiments presented by Hansen and Ingason [1] as these tests were found to fit very well to the aim of the work presented here. The purpose of this paper is to describe the fire behaviour and its impact on the surroundings during a fire with multiple fuel items on fire in a mine drift with longitudinal ventilation. Better knowledge about fire behaviour is needed for underground hard rock mines [2] and as the number of studies in the field are generally limited to open space cases or cases with only natural ventilation the need for this knowledge is further underlined.

A number of studies have been conducted on the fire behaviour of merging flames from multiple fires in open space [3-5]. The individual flames will merge into a single flame with longer flame length when placed sufficiently close together. This is due to the reduction of air entrainment due to the adjacent fires which will cause a pressure gradient resulting in flames leaning towards each other and finally merging. The flame length will increase substantially with a decreasing distance when the flames start to emerge, but after the flames are fully merged the distance between the fires will have little effect on the flame length. The studies have been conducted on fires with natural ventilation, using fire sources such as gas burners, pool fires and wood crib fires.

As opposed to fires in the open, multiple fires in a mine drift or a tunnel will be affected by the surrounding surfaces. Wan et al [6] performed a number of fire experiments in a model scale tunnel with two propane burners acting as separate fires. During the experiments the heat release rate and distance between the burners were varied. It was found that the spacing between the gas burners had a more significant effect on flame length in open space than in a tunnel. A criterion of beginning merging and fully merging flames were proposed. Models for predicting the ceiling gas temperature profiles and flame lengths were presented. Ji et al [7] presented a study where experiments with two pool fires in a model scale tunnel were conducted, studying the interaction between the fires as the heat release rates and distance between the fires were varied. The mass loss rate of the fires was found to initially increase and then decrease as the distance was increased. The maximum mass loss rate was found to occur at a shorter distance between the fires in a tunnel compared with the open case. The mass loss rate of a pool fire - with an adjacent pool fire in a tunnel - was higher than the corresponding case in the open. No forced, longitudinal ventilation was used during either of the studies.

It is somewhat troublesome and doubtful to draw any extensive conclusions based upon experiments conducted with pool or gas burner fires on the fire behaviour for fires in a mine drift, as these fires will often be fires in solid materials, with varying heat release rates, varying flame spread, varying flame lengths and where the re-radiation to the fuel surface will have an influence on the fire development (as opposed to gas burner fires).

Ingason [8] performed a number of model scale fire experiments simulating a tunnel fire involving several HGV trailers, using wood cribs as fire load. The main purposes of the work were to investigate the effects of variable ventilation rate on the maximum heat release rate and fire growth rate. It was found that an increase in the ventilation rate lead to an increase in the maximum heat release rate per unit fuel are which was 1.4 to 1.55 times higher than the corresponding open fire case. The increase in the fire growth rate was 2 to 3 times higher when increasing the ventilation rate to 3 m/s and 5 m/s respectively. The influence of the longitudinal ventilation on the heat release rate of ventilation controlled fires will have an even further impact where the porosity factor will be a key parameter.

Hansen and Ingason [1] [9] presented studies focusing on the ignition of individual fuel items and the calculation of the heat release rate of multiple objects located in an underground structure. The output of the calculations were compared to model scale fire experiments with varying number of wood cribs and pallets placed at equal distances as well as varying distances from the ignited wood crib and the pile of wooden pallets. The experiments were performed in a model scale mine drift/tunnel with longitudinal ventilation.

In the following, the general fire behaviour of a single fire source in a mine drift is outlined and discussed, model scale experiments by Hansen and Ingason [1] are described and the results of the model scale experiments are presented and analysed with respect to the fire behaviour and the impact on the surroundings.

2. General fire behavior in a mine drift – single fire source

The fuel load in an underground mine can be considerable at specific and isolated positions. Positions with a more or less continuous, spatial distribution of combustible items could for example be a mine drift used as a parking lot for larger mining vehicles. The fuel load in a mine drift will mostly be found in the lower regions and will therefore not necessarily be engulfed in hot fire gases or largely affected by ceiling impingement of flames, thus limiting the effect of the fire spread mechanisms [2].

Several different types of combustibles can be found in a mine drift depending on the type of activity. Types of combustibles could for example be: vehicles, flammable liquid, wooden pallets, electrical cables, tyres, hoses, conveyor belts etc.

Vehicle fires are the most common type of fire in underground hard rock mines [10-11] and may result in high heat release rates and extensive smoke spread. The maximum heat release rate of larger mining vehicles can be several tens of megawatts, putting the fire protection systems in a mine to the test and causing great problems and risks to the personnel in the mine. Depending on the type of vehicle the fuel load and construction will vary, but generally combustibles such as tyres, flammable liquids, cables and hoses are found on the vehicles.

Fires in flammable liquids can be characterized by the rapid fire growth; considerable and rapid smoke production.

Fires in tyres and larger amounts of hydraulic hoses are distinguished by the extensive smoke production and the long fire duration which will increase the risk to evacuating miners. The heat release rates of fires in tyres, cables, hoses and other solid materials will be dictated by the size of the involved surface area at the time.

A fire in a mine drift will either be ventilation controlled or fuel controlled. The heat release rate of a ventilation controlled fire will be dictated by the amount of oxygen available (i.e. there is no excess of oxygen) and the amount of fuel will dictate the heat release rate of a fuel controlled fire. The following equation is used for determining whether the fire is ventilation controlled or fuel controlled [12]:

$$\phi = 3000 \cdot \frac{\dot{m}_a}{\dot{Q}} \qquad (1)$$

The fire is fuel controlled if equation (1) is larger than 1. Due to the generally large dimensions of a mining drift and the presence of longitudinal ventilation, a fire in a mine drift will in most cases be a fuel controlled fire.

Unshielded flames in a mine drift are affected by the longitudinal ventilation flow from the mechanical ventilation, which can visually be seen in the tilting of flames. Tilting flames lead to faster flame spread, higher fire growth rate, higher maximum heat release rates and faster ignition of adjacent fuel as the view factor will increase and flame impingement may occur as well. The following flame tilt angle relationships of Li and Ingason [13] were developed for tunnel fires with longitudinal ventilation and validated against model scale as well as large scale fire experiments:

$$\sin\varphi = 1 \qquad V' \le 0.19 \qquad (2)$$

$$\sin\varphi = (5.26 \cdot V')^{-3/5} \qquad V' > 0.19 \qquad Q^* \le 0.15 \qquad (3)$$

$$\sin\varphi = 0.25\cdot\left(\frac{D}{2}\cdot V^{*3}/H\right)^{-1/5} \qquad V' > 0.19 \qquad Q^* > 0.15 \tag{4}$$

$$V' = \frac{u}{w^*} \tag{5}$$

$$w^* = \left(\frac{g\cdot\dot{Q}}{\frac{D}{2}\cdot\rho_a\cdot c_p\cdot T_a}\right)^{1/3} \tag{6}$$

$$V^* = \frac{u}{\sqrt{g\cdot H}} \tag{7}$$

$$\dot{Q}^* = \frac{\dot{Q}}{\rho_a\cdot c_p\cdot T_a\cdot g^{1/2}\cdot H_f^{5/2}} \tag{8}$$

The flame length will also play an important part with respect to the spread of fire to adjacent items due to the importance of the flame radiation mechanism. The following correlations of Ingason and Li [14] have been found to match observed non-dimensional flame lengths from performed full-scale fire experiments in a mine drift [15]:

$$L_f^* = 4.3\cdot\dot{Q}_f^* \tag{9}$$

$$L_f^* = \frac{L_f}{H} \tag{10}$$

$$\dot{Q}_f^* = \frac{\dot{Q}}{\rho_a\cdot c_p\cdot T_a\cdot g^{1/2}\cdot A\cdot H_f^{1/2}} \tag{11}$$

The mine drift geometry is accounted for in the correlations above, which underlines the influence of the geometry on the flame lengths in a mine drift.

As the longitudinal ventilation flow increases, the flame lengths and flame temperatures in a mine drift will decrease due to increased air entrainment which will increase the combustion efficiency. The initial increase in the heat release rate and fire growth rate due to increased longitudinal ventilation flow will eventually reach a maximum value at a certain ventilation velocity. A further increase in the ventilation velocity will result in a decrease in the heat release rate and fire growth rate as the convective cooling overtakes the radiative heating from the flames. In figure 1 the measured incident heat flux at floor level in a model scale mine drift/tunnel fire experiment can be seen. The experiments are described further in the coming chapter. The heat flux was measured 1 m downstream of a burning pile of wooden pallets at three different ventilation velocities. As can be seen, a higher maximum heat flux was measured for the 0.6 m/s case compared with the 0.3 m/s and 0.9 m/s cases. The ventilation velocities of the model scale experiments equal 1.16 m/s, 2.32 m/s and 3.49 m/s respectively in full scale.

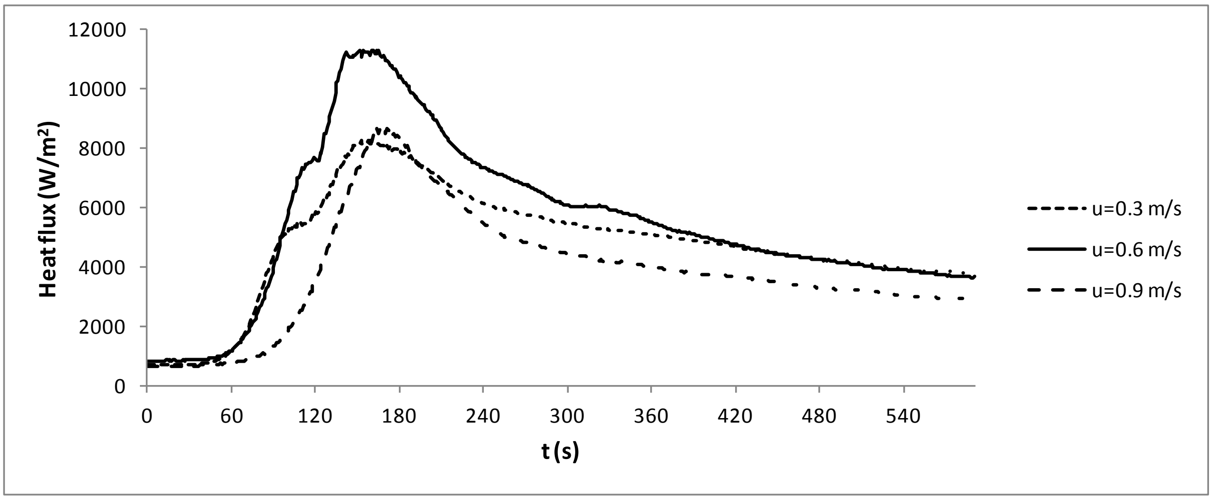

Figure 1. Heat fluxes at different ventilation velocities in model scale fire experiments.

The dominating fire spread mechanism will vary with the distance from the fire, the position of the fuel items with respect to the ventilation flow direction as well as the spread of the fire gases, and type of material involved in the fire.

For shorter distances the flame radiation will play a crucial part with respect to spread mechanisms. Thus the flame radiation mechanism will be very important during the fire spread between the various fuel components of a vehicle. The convective heat transfer mechanism will increase in importance with increasing distance.

The ventilation flow may push the fire gases away from an adjacent fuel component, thus decreasing the impact of the convective heat transfer term. On the other hand, a longitudinal ventilation flow will tilt flames towards adjacent fuel items and increase the importance of the flame radiation transfer term.

The mine drift itself will also influence the fire behaviour. The surrounding rock close to the fire will increase the re-radiation mechanism back to the fire and increase the heat release rate. The rock further downstream of the fire will instead have a cooling effect on the fire gases and therefore decrease the stratification of the smoke and the risk of ignition of fuel items downstream. The mine drift height will in many cases be considerable, decreasing the risk of ceiling impingement of flames. The inclination of the mine drift will also influence the fire behaviour, where the inclination will lead to increasing flame tilt which in turn will lead to earlier ignition of fuel items, faster flame spread etc.

The general openness and cooling effect of a mine drift - together with the generally limited amount of combustible material - will decrease the likelihood of a flashover. Even though a flashover is less likely to occur; severe, fast spreading and high intensity fires are not unlikely. A mine drift with a continuity of large amount of combustibles could very well be the place of a large and dangerous fire.

The smoke spread in a mine drift is largely determined by the longitudinal ventilation flow. The longitudinal ventilation velocity will determine the occurring smoke stratification, together with the dimensions of the mine drift, the heat release rate as well as the distance to the fire. With a low or no forced air velocity the smoke stratification will be high in the vicinity of the fire and at high air velocities the smoke stratification will be low downstream from the fire. With increasing mine drift height and increasing distance to the fire, the vertical temperature gradients as well as the smoke stratification will decrease. An increase in the heat release rate will result in an increase in the vertical temperature gradients and the smoke stratification. Figure 2 displays the smoke stratification along a mine drift, where the vertical temperature gradient, stratification as well as average fire gas temperature decrease with increasing distance from the fire.

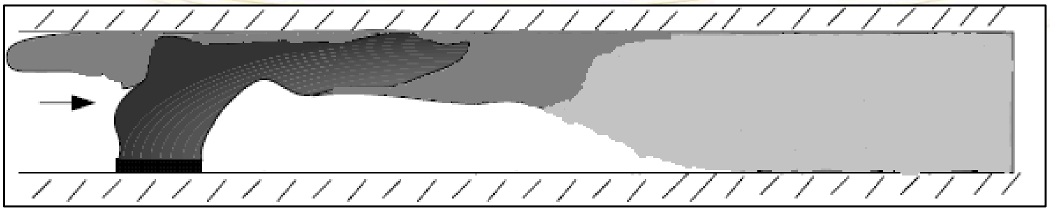

Figure 2. The smoke stratification in a mine drift for a single fire source [2].

3. Performed model scale fire experiments

In the following a brief summary of the performed fire experiments is presented. For a more detailed description of the wooden pallets, the experimental procedures and heat release rate results of the experiments see Hansen and Ingason [16].

Hansen and Ingason [1] presented a series of model scale mine drift/tunnel fire tests, carrying out a total of 12 tests in a 1:15 model scale tunnel (the size of the tunnel was 10 m long, 0.6 m wide and 0.4 m in height). The parameters tested during the tests were: the distance between piles of wooden pallets and longitudinal ventilation rate (longitudinal ventilation velocities of 0.3 m/s, 0.6 m/s and 0.9 m/s were applied during the experiments). The aim of the study was to investigate the effect of varying distances between the wooden pallet piles on fire spread under different longitudinal ventilation rates. See figure 3 for a sketch of the model tunnel and figure 4 for the position of thermocouples, probes and instruments.

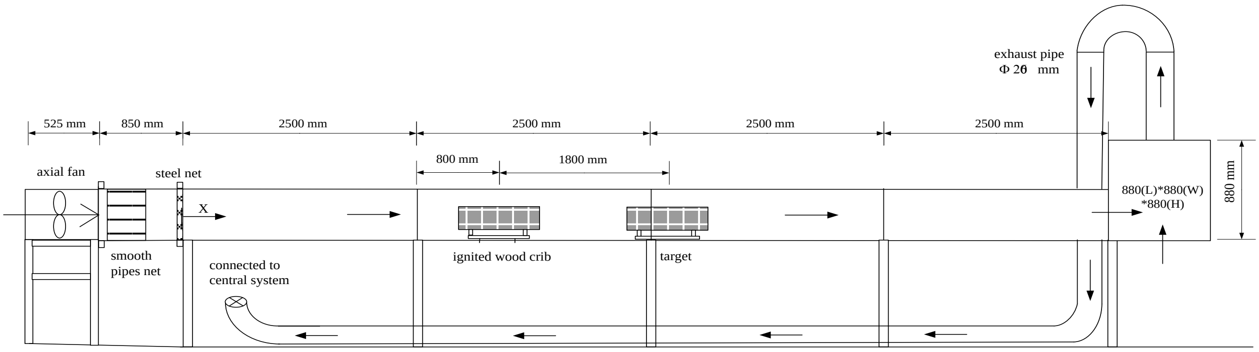

Figure 3. A schematic drawing of the model tunnel [8].

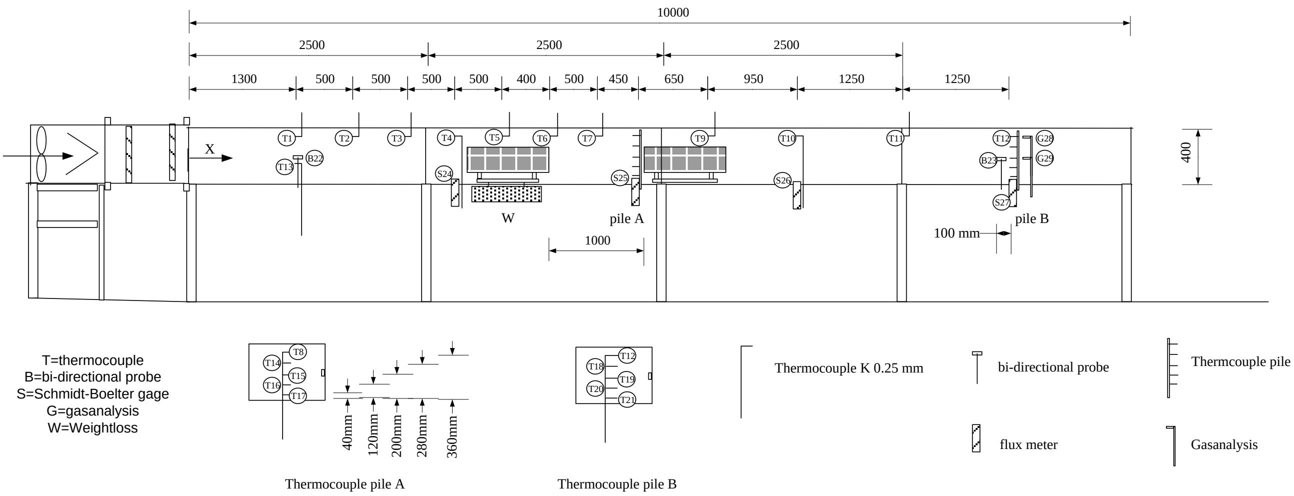

Figure 4. Position of thermocouples, probes and instruments [8].

The applied fire load in the experiments consisted of piles of scaled down softwood pallets (pine), where each pile was composed of five individual wooden pallets. Three test fires were used as reference tests and consisted of a single pile of pallets, whereas in the other tests the fire load consisted of four piles of wood pallets placed at different distances between each other.

During the tests the following parameters were measured or calculated:

> Time of ignition of adjacent piles were clocked and documented manually.

> The total heat release rate.

- Fire gas temperatures; where most of the thermocouples were placed along the ceiling. Two sets of thermocouples were also positioned 4.65 m and 8.75 m from the inlet opening, measuring the temperatures at various vertical positions from which an average fire gas temperature could be calculated.
- Gas concentrations at the end of the tunnel.
- Heat fluxes at floor level at several positions.
- The centreline flow velocity.
- The centreline pressure difference.

All experiments were visually documented using a video camera, recording the fire behaviour along the long side of the tunnel. The long side of the tunnel was covered with a fire resistant 5 mm window glaze, allowing for visual observations of ignition, flame lengths, tilting flames etc. See table 1 for the results from the model scale experiments. Experiment #2 comprised of four piles of wooden pallets but where only the initial pile took part in the fire and was therefore not included in the analysis. The ignition time of the first pile of wooden pallets was set to 0 s.

Table 1. Results from the model scale fire experiments.

Test #	u [m/s]	Number of piles	Free distance between the piles [m]	Maximum heat release rate [kW]	Ignition times of second and third pile [s]	Engulfment times of first, second and third pile [s]	Time after ignition when flames became horizontal [s]	Heat release rate when flames became horizontal [kW]	Measured continuous flame lengths [m]	Heat release rate at measured continuous flame lengths [kW]
1	0.3	1	-	116	-	-	-	-	-	-
3	0.6	4	0.4; 0.7; 0.6.	504	96; 129	58; 131; 161	139	359	1.09	170
									1.73	222
									2.67	364
4	0.6	1	-	154	-	-	-	-	-	-
5	0.6	4	0.5; 0.7; 0.8.	467	111; 164	73; 158; 188	164	285	1.09	160
									1.73	184
									2.67	318
6	0.6	4	0.5; 0.8; 0.9.	488	105; 149	63; 142; 168	146	249	1.73	154
									2.67	324
									2.67	324
7	0.6	4	0.5; 0.8; 1.1.	485	96; 139	66; 140; 162	142	320	1.73	171
									2.67	281
									3.91	452
8	0.6	4	0.5; 0.8; 1.3.	479	99; 140	60; 135; 160	140	231	1.09	157
									1.73	172
									3.91	440
9	0.6	4	0.6; 0.8; 1.1.	461	110; 162	58; 144; 176	151	216	1.73	183
									2.67	331
									3.91	422
10	0.6	4	0.7; 0.8; 1.1.	454	130; 183	58; 166; 218	168	195	-	-
11	0.6	4	0.7; 0.9; 1.1.	464	134; 196	62; 177; 229	172	205	1.09	145
12	0.9	1	-	169	-	-	-	-	-	-

The use of model scale fire experiments is convenient as it allows for less costly experiments where the results can be translated into a full scale system, using the theory of dimensionless groups as a basis. A relatively well defined similarity exists between model scale and full scale experiments.

The size of the model scale mine drift was scaled geometrically according to a 1:15 ratio. The scaling models of the heat release rate, flow rate, time, energy content, mass and temperature, can be found in table 2. The index *F* relates to the full scale (i.e. 15 in our case) and the index *M* relates to the model scale (i.e. 1 in our case).

The influence of the thermal inertia of the involved material, the turbulence intensity and radiation was neglected.

Table 2. List of scaling models [8].

Unit	Scaling model	Equation number
Heat release rate [kW]	$\dot{Q}_F = \dot{Q}_M \cdot \left(\frac{L_F}{L_M}\right)^{5/2}$	(12)
Velocity [m/s]	$u_F = u_M \cdot \left(\frac{L_F}{L_M}\right)^{1/2}$	(13)
Time [s]	$t_F = t_M \cdot \left(\frac{L_F}{L_M}\right)^{1/2}$	(14)
Energy [kJ]	$E_F = E_M \cdot \left(\frac{L_F}{L_M}\right)^{3} \cdot \frac{\Delta H_{c,M}}{\Delta H_{c,F}}$	(15)
Mass [kg]	$m_F = m_M \cdot \left(\frac{L_F}{L_M}\right)^{3}$	(16)
Temperature [K]	$T_F = T_M$	(17)

4. Results and discussion of fire experiments

A fire in a mine drift involving multiple separate fires and with longitudinal ventilation will be complex and affected by numerous factors: flame tilt, varying degree of air entrainment depending on the position of the fire versus the other fires and the ventilation direction, distance between the fires, number of fires, heat release rates of the individual fires, fire interaction, effect of surrounding surfaces and dimensions of the mine drift, orientation of fuel surfaces versus ventilation flow, flow of fire gases and flames etc. In some cases the various factors will affect each other and further complicate the fire behaviour.

4.1 Fire gas temperatures

A fire gas layer temperature criterion of 600°C - which is a flashover criterion for remote ignition [17] - was applied at roof level to study the extent of the fire gas layer with flashover potential. In figure 5 the roof temperatures for the thermocouples in experiment #7 that exceeded 600°C can be seen. The fire gas layer with flashover potential will not be stationary, instead it will move in the direction of the ventilation flow. Also, the extent of the layer will initially increase with each pile of pallets being ignited and then gradually decrease as the number of piles is limited. A spatial continuity in the combustible material is essential to allow the flashover conditions to increase and progress along the mine drift/tunnel. The span of distances between the piles of pallets in the model scale experiments (0.4 m -- 1.1 m) correspond to a span between 6 m and 16.5 m in full scale. Figure 6 displays the roof temperatures of experiment #4 where the fire gas layer temperature exceeded 600°C. Comparing with figure 5, it is clear that the extent of the zone where flashover may occur is limited - both in time and space - compared with experiment #7 due to the lack of continuity in combustible material. Even though it is generally less likely that a flashover would occur in a mine drift compared with a fire in an enclosure, the experiments clearly show the possibility given the right circumstances. A flashover in an open mine drift would not include the entire mine drift at one time, but would instead have a limited spatial extent and non-stationary characteristics. The extent of the zone where flashover may occur was 16.5 m (full scale) downstream of the last pile of pallets in experiment #7.

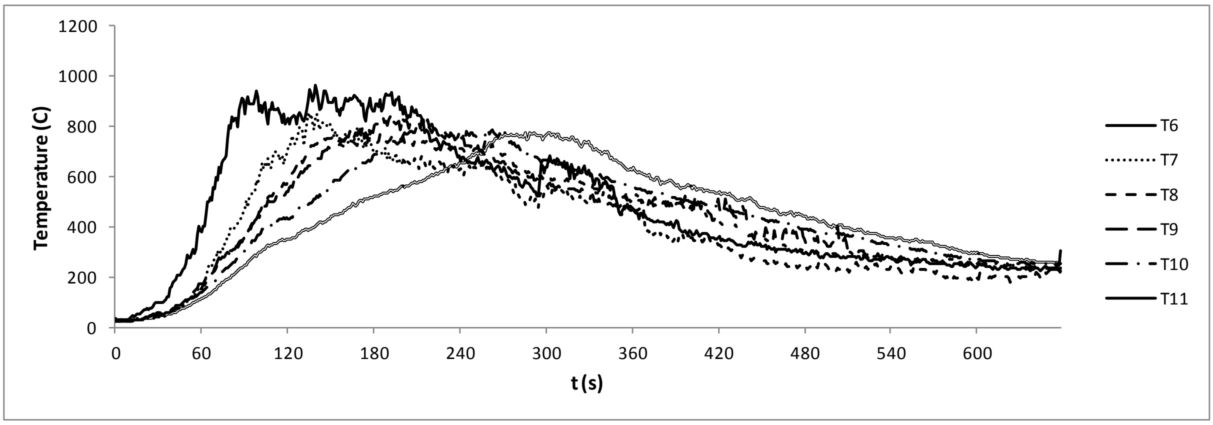

Figure 5. The roof temperatures of thermocouples exceeding 600°C in experiment #7.

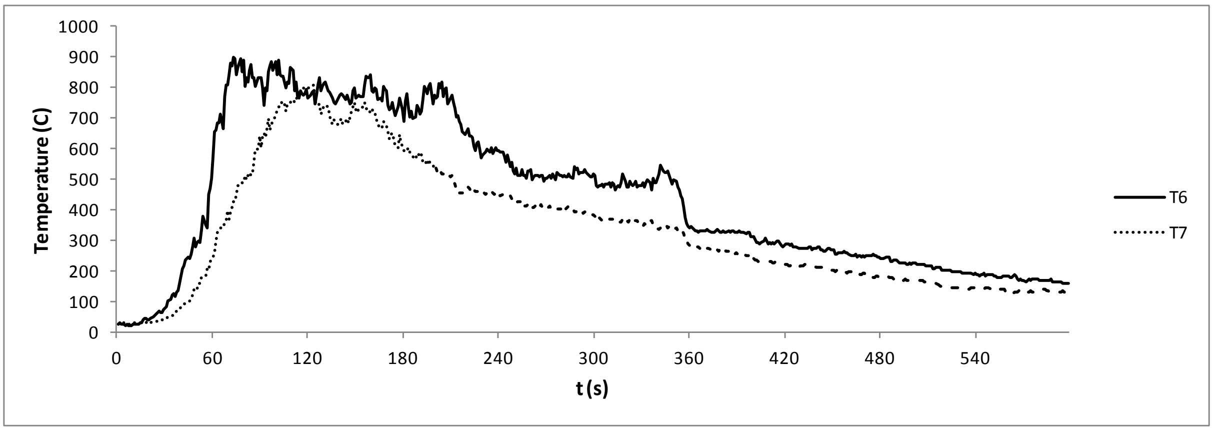

Figure 6. The roof temperatures of thermocouples exceeding 600°C in experiment #4.

The temperature readings at pile A in experiment #4 can be seen in figure 7. The experiment only involved one pile of pallets. As noted there is a distinct temperature gradient between the lower two thermocouples and the upper three thermocouples. A clear stratification resulted from the experiment during a majority of the fire except at the very end.

The corresponding temperature readings of experiment #7 can be seen in figure 8. As opposed to the temperature readings from experiment #4, the temperatures of experiment #7 display a period subsequent to the early growth phase and prior to the decay phase, where the temperature gradient is very low and resulting in very little stratification. The lowest thermocouple (T17) in figure 7 displays a temperature that starts to level out after approximately 90 seconds, while the same thermocouple in figure 8 displays a temperature that continues to increase more and more. At this point of time, the second pile of wooden pallets was ignited in experiment #7 while experiment #4 only involved one pile total. Thus the fire of experiment #7 continued to increase in intensity and temperature due to the continuation of combustible material.

In figure 8 the period with little stratification is initiated when temperature readings of the two lowest thermocouples (T16 and T17) start a very rapid climb after about 150 s. Studying the video recordings from the experiment, it was seen that the fire had spread to the lower parts of the second pile and the flames started to tilt more or less horizontally at this time, directed towards the thermocouples of pile A.

Figure 9 displays the temperature readings of pile B in experiment #11, where the last pile of pallets was positioned closest to pile B (approximately 2.1 m, which equals 31.5 m in full scale) among all experiments. Same as for experiment #7, figure 9 displays a period with smaller temperature gradient and thus less stratification. This period starts after approximately 280 s where the lowest thermocouple (T21) initiates a rapid increase in temperature. Studying the video recordings, the same phenomenon occurs as in experiment #7 where the pile of pallets closest to pile B is ignited shortly before and the flames toward pile B is tilted horizontally even from the lower parts of the pile.

The model scale experiments displayed a different temperature distribution and stratification along the mine drift compared with the case of only one fire source (seen in figure 2). Instead of a clear temperature gradient and a clear stratification, the experiments showed a more or less uniform vertical temperature distribution - with high temperatures - and little stratification for a considerable distance along the model scale mine drift.

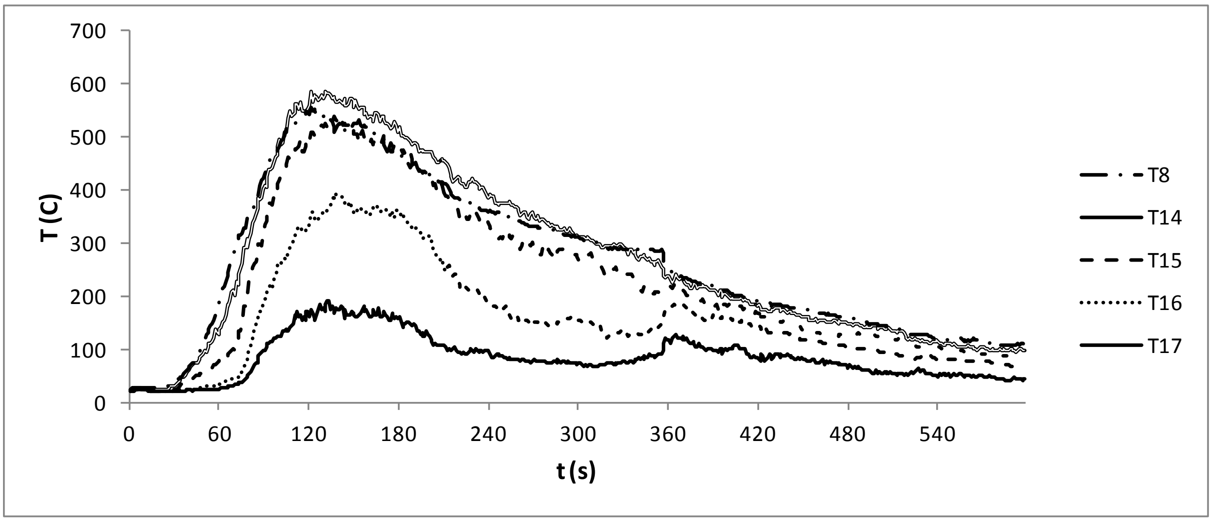

Figure 7. The temperature readings at pile A in experiment #4.

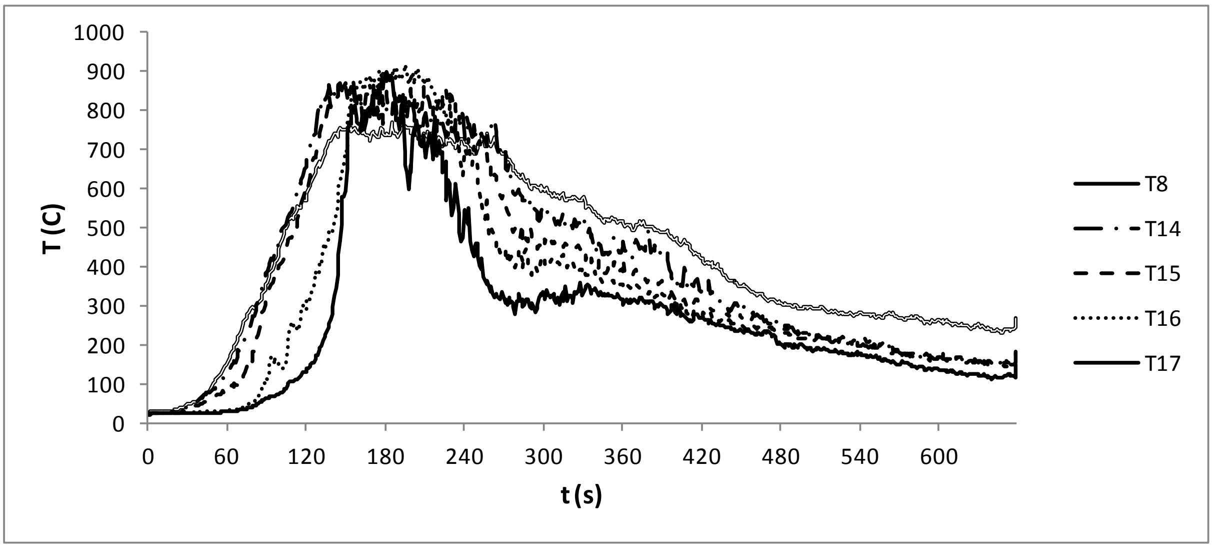

Figure 8. The temperature readings at pile A in experiment #7.

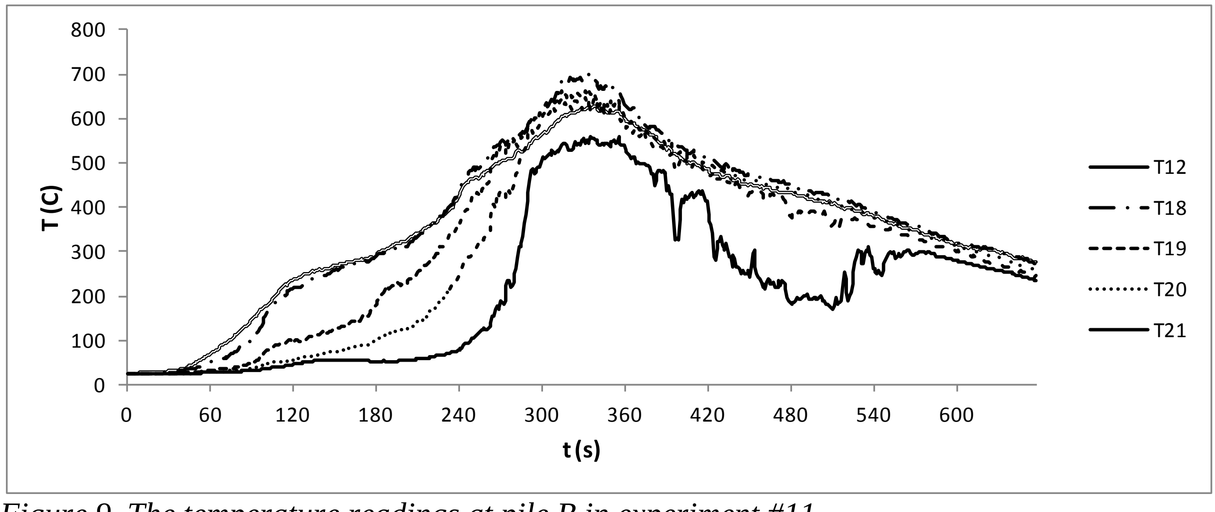

Figure 9. The temperature readings at pile B in experiment #11.

4.2 Flame behaviour

During the experiments with multiple fires, it was found that during all experiments did the flames tilt horizontally and filled up the entire cross section (see figure 10). Applying equations (2)-(8) for the model scale experiments, the results did not predict horizontal flames. This is not surprising as Li and Ingason [13] focus on the ceiling temperature when predicting the tilt of the flames and will not give any clues on the temperatures and flame tilts closer to the ground. Also, for very large fires the flame volume would be across the entire cross section and not only at the ceiling.

Figure 10. The flame volume across the entire cross section in experiment #5.

When studying the video recordings of the experiments it could be seen that cut-off – ceiling impingement - of the flames occurred for the first pile of pallets. But as the flames started to tilt horizontally for the subsequent piles, the ceiling impingement more or less ceased.

Studying the video recordings from the experiments, the flames did not fully merge with each other (other than very occasionally and only at the very top and base). Instead they tied into each other, forming a more or less continuous flame along the mine drift due to the longitudinal ventilation flow and flame volume across the entire cross section.

When trying to visually observe the individual flame lengths of the piles of wooden pallets it was found to be difficult due to the soot that covered the flame tip, soot on the window glaze and the fluctuating nature of the flame tips. Instead the flame length at the various thermocouples positioned along the mine drift and pile A and B was determined by using the temperature readings of the various positions, assuming a flame tip temperature of 500 K above ambient and that the continuous flame has reached pile A or B when the temperature at any of the thermocouple is constantly above 500 K of ambient [18]. See table 1 for the measured continuous flame lengths and corresponding heat release rates of the experiments.

The measured flame lengths indicated increasing and longer flame lengths with each ignited pile of pallets further downstream (when comparing with the flame length of the reference test). Figure 11 displays the continuous flame lengths of experiment #4 (reference test) and #7 as a function of time until the maximum flame length was attained. The maximum continuous flame length of experiment #7 was more than four times larger than the maximum flame length of experiment #4 even though the maximum continuous flame length of experiment #7 only encompassed three piles of wooden pallets. The longitudinal ventilation flow will increase the combustion efficiency of the first pile of wooden pallets, resulting in increased heat release rate and fire growth rate, and decreasing flame lengths and flame temperatures for the first pile. But further downstream the air entrainment will decrease with each fuel item, resulting in increased flame lengths and flame temperatures which in turn will lead to earlier ignition of adjacent fuel items. The fire growth rate and heat release rate of fuel items further downstream will still increase – despite decreased air entrainment – as more fuel items will be ignited at an earlier stage of the fire and a larger portion of the fuel surface of each fuel item will be ignited at an earlier stage due to flames tilted horizontally and filling up the entire cross section. This will increase in importance as the distance between the fires decrease and the number of fires increase.

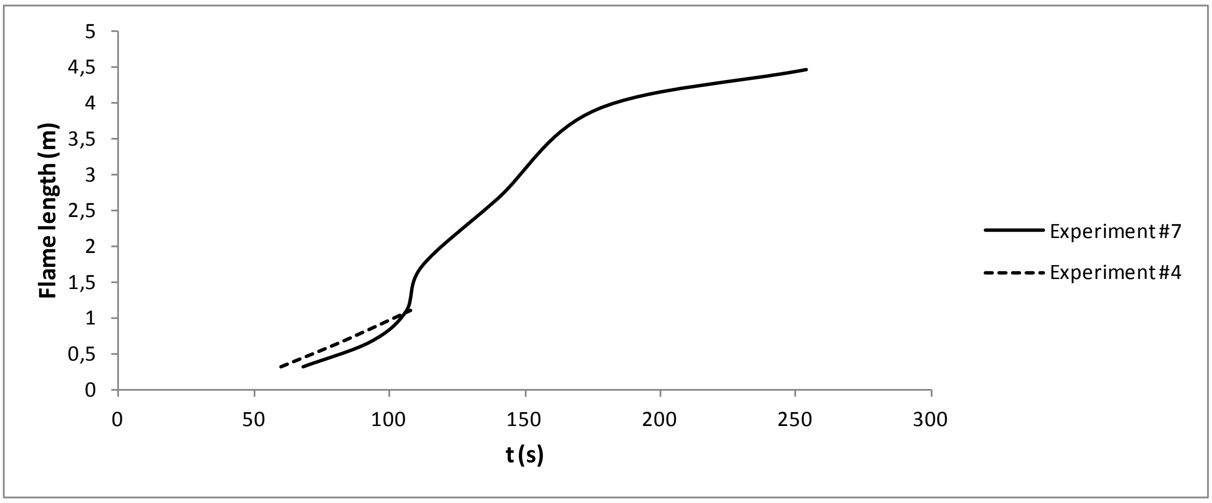

Figure 11. The flame length developments of experiment #4 and #7.

When applying equations (9)-(11) for calculating the flame lengths, it was found that the calculated flame lengths were considerably longer than the measured flame lengths (see figure 12 for the calculated and measured flame lengths of experiment #3). The use of the flame length correlations of Ingason and Li [14] would in this case seem to fit a single fire source better than for multiple fire sources. A possible explanation could be that the air entrainment for several fire sources would be more efficient than the air entrainment of a single fire source with the same heat release rate, thus resulting in a longer flame length for a single fire source.

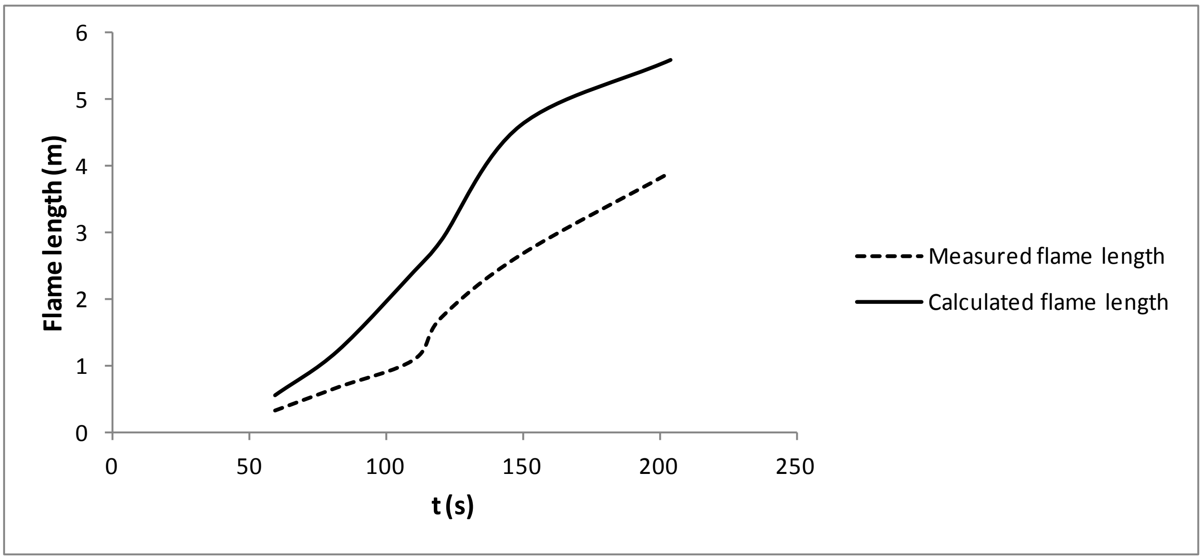

Figure 12. Flame lengths of experiment #3.

Applying dimensional analysis on the continuous flame length along the model scale mine drift, the following governing parameters were included based upon earlier studies [3], [7], [19], [20]:

$$L_f = f\left(\dot{Q}, \rho_a, c_p, T_a, g, H_f, S\right) \quad (18)$$

An earlier paper by Ingason and Li [14] had found that the flame length was only a weak function of the longitudinal ventilation flow and was therefore not included in the dimensional analysis.

Furthermore, when analyzing the model scale fire experiments it was found that the fuel diameter did not play a significant role when determining the flame length due to the long flame lengths encountered for multiple fires. The fuel diameter was therefore also excluded from the dimensional analysis.

The normalized flame length:

$$\frac{L_f}{S} = f\left(\frac{\dot{Q}}{\rho_a \cdot c_p \cdot T_a \cdot g^{1/2} \cdot S^{5/2}}, \frac{H_f}{S}\right) \quad (19)$$

$$\frac{L_f}{S} = f\left(\frac{\dot{Q}}{\rho_a \cdot c_p \cdot T_a \cdot g^{1/2} \cdot S \cdot H_f^{3/2}}\right) \quad (20)$$

Setting the dimensionless heat release rate equal to:

$$\dot{Q}^* = \frac{\dot{Q}}{\rho_a \cdot c_p \cdot T_a \cdot g^{1/2} \cdot S \cdot H_f^{3/2}} \quad (21)$$

Performing a regression analysis on the measured flame lengths for various total heat release rates and average free distances between the piles of wooden pallets (as the distances varied in the same experiment), resulted in the following correlation:

$$L_f = 1.61 \cdot S_{avg} \cdot \dot{Q}^* \qquad (22)$$

The plotting of the correlation between the normalized flame length and normalized heat release rate can be seen in figure 13. A R^2 value of 0.892 resulted, showing that the continuous flame length can be reasonably well described by using equation (22). The high correction coefficient value further motivates the exclusion of the longitudinal ventilation flow and fuel diameter from the dimensional analysis.

Equation (22) expresses the continuous flame length of multiple fires in a mine drift with longitudinal ventilation flow. Cases with several separate flames are not accounted for in equation (22).

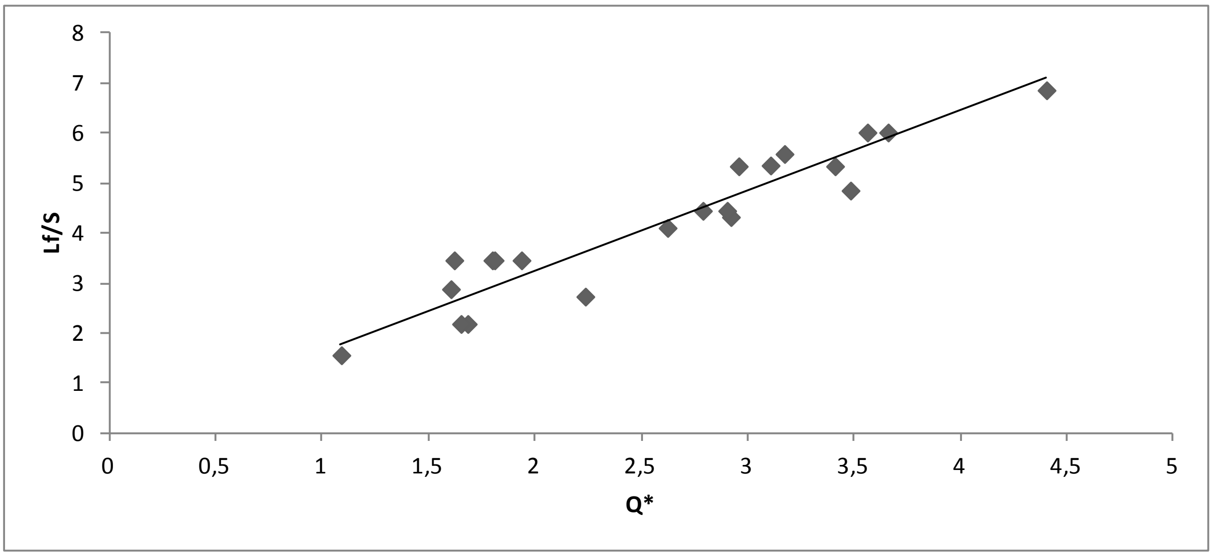

Figure 13. Correlation of normalized flame length against normalized heat release rate.

4.3 Spread mechanisms

The main fire spread mechanisms in all experiments were convection, flame radiation and flame impingement, but the difference lays in the size of the fuel area being affected as a function of the time. Figure 14 displays the moment just before ignition of the second pile of wooden pallets of test fire #5, as can be seen flame radiation will affect the entire side and upper surface of the pile but mostly the upper part due to the tilted flame. Convection and flame impingement will mostly affect the upper part of the pile. Figure 15 displays the moment where the third pile of wooden pallets of test fire #5 is ignited. As can be seen, convection, flame radiation and flame impingement will affect the entire side of the pile as well as the upper surface. Even though the upper part of the pile is ignited first, the entire side of the pile will ignite more or less momentarily shortly afterwards. Thus a larger fuel surface area will be on fire at an early stage, leading to a faster fire growth rate and a higher maximum heat release rate.

A fire scenario with fuel surfaces at the lower regions of the mine drift being exposed to a larger degree of convection, flame radiation and flame impingement may have a severe impact on the fire safety. This is due to the fact that the larger amount of combustible materials is found in the lower regions of the mine drift [2] and the fire protection measures in the mine drift may not have been addressed with respect to such fire behaviour.

Figure 14. Photograph taken just before ignition of the second pile of wooden pallets of test fire #5.

Figure 15. Photograph taken at the ignition of the third pile of wooden pallets of test fire #5.

4.4 Fire growth rate and fire spread rate

The heat release rate of the reference test was subtracted from the total heat release rate of the other experiments in order to analyse the heat release rate of the second pile of wooden pallets, assuming that the heat release rate of the reference test was similar to the heat release rate of the first pile in the different tests. The fire growth rate and heat release rate of the second pile of wooden pallets were examined and compared with the corresponding values of the first pile, from the ignition of the pile until the time when the third pile was ignited. The resulting heat release rate from experiment #9 can be seen in figure 16. As can be seen the fire growth rate as well as the heat release rate increased dramatically for the second pile.

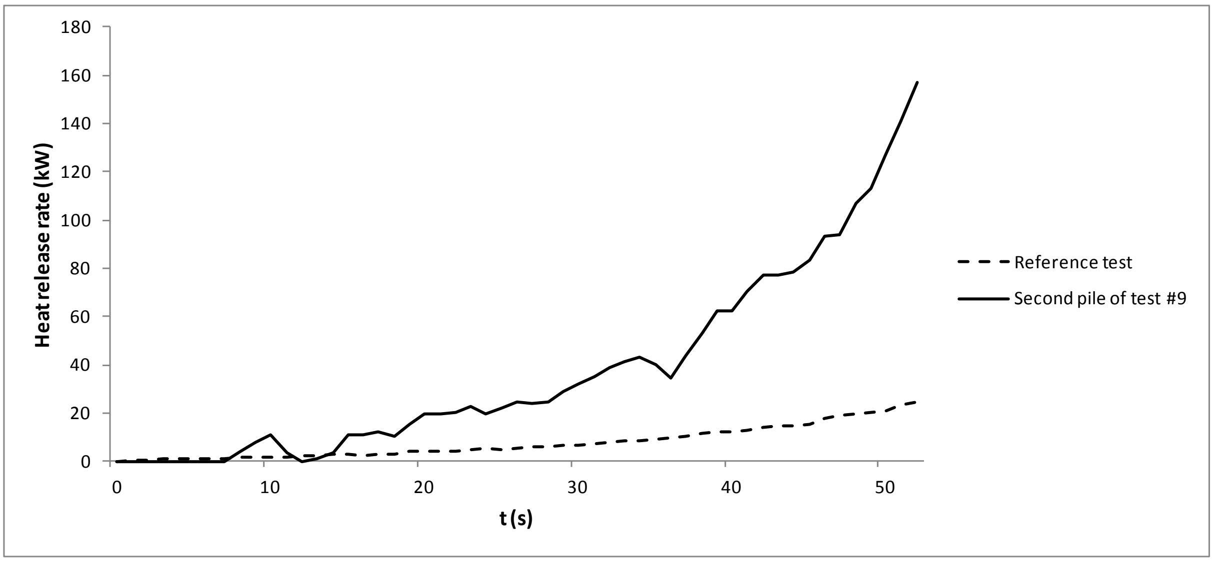

Figure 16. The initial heat release rate of the reference test and the second pile of experiment #9.

The resulting fire growth rates (a parabolic growth rate was applied as the fire growth rates had a parabolic appearance) and heat release rates can be seen in table 3. As can be seen, the fire growth rate of the second pile increased with decreasing distance between the first and second pile. The fire growth rate and heat release rate (at t=30 s after ignition) were considerably higher for the second pile compared with the reference test of the first pile. Indicating an increasing fire growth rate, more rapid ignition, higher maximum heat release rate, escalating fire severity, worsening fire behaviour with increasing number of adjacent combustible items downstream of the fire.

Table 3. Fire growth rates and heat release rates of the reference test and the second pile of the experiments with multiple piles of wooden pallets.

Experiment #	**Parabolic fire growth rate [kW/s^2]**	**Heat release rate at t=30 s [kW]**	**Free distance between first and second pile [m]**
3	0.081	86	0.4
4 (reference)	0.009	7	-
5	0.037	22	0.5
6	0.048	46	0.5
7	0.056	71	0.5
8	0.044	49	0.5
9	0.058	32	0.6
10	0.038	47	0.7
11	0.032	37	0.7

Using the heat release rate curve of the reference test (#4), adding the curve at the recorded ignition times of the individual piles and summing it up into a total heat release rate of the experiment in question, figure 17 displays the summed up heat release rate of experiment #3 and the measured heat release rate. As can be seen, the measured heat release rate displays a more rapid fire growth rate after the initial phase (where only the first pile was involved in the fire) compared with the summed up heat release rate, showing that the fire growth rate of the second, third and fourth pile was higher compared with the first pile.

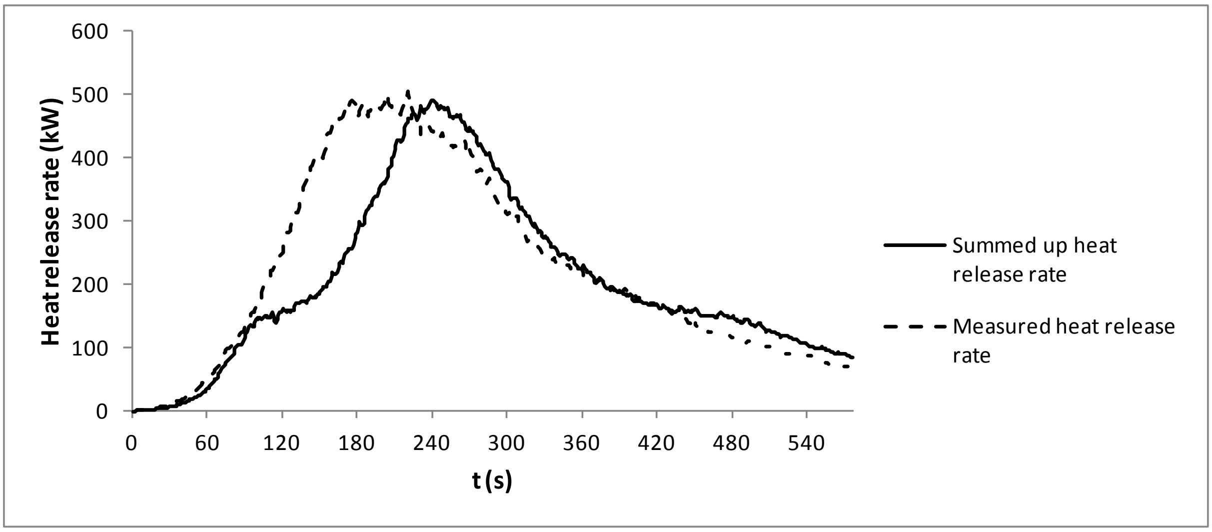

Figure 17. The summed up heat release rate and measured heat release rate of experiment #3.

The video recordings from the experiments were studied in order to obtain approximate times from ignition of a pile and until the pile was fully involved in the fire. The pile was assumed to be fully involved in the fire when flames were seen flowing from the bottom to the top of the pile on the downstream side. Due to soot formation on the window glaze it was difficult to observe flames emitted from the fourth pile of pallets and the results of the fourth pile was therefore omitted. See table 1 for the ignition times and times of engulfment for the experiments. The average time duration - from ignition to fully involved fire - was 62 s (standard deviation of 5.2) for the first pile, 39 s (standard deviation of 4.9) for the second pile and 25 s (standard deviation of 7.5) for the third pile. Thus a decreasing time duration and an increasing fire growth rate for each additional pile downstream of the initial fire. Please observe that the first pile was ignited at the bottom of the pile and the buoyancy clearly facilitated the flame spread along the pallet surfaces. In the case of the second pile, the pile was ignited at the top and the flame spread was not assisted by the buoyancy. The time difference between the first and second pile should therefore have been larger if the ignition point would have been identical in both cases.

The measured heat flux values at the floor level were studied in order to obtain approximate values of the fire spread along the mine drift/tunnel. A heat flux criterion of 13.1 kW/m^2 was set based upon the critical heat flux of the wooden pallets [1]. The fire was assumed to reach the position of the flux meter when the measured heat flux exceeded the critical heat flux. It was found that the fire accelerated considerably during the course; three to four times higher spread rates were measured between the second and third heat flux meter compared with the spread rate between the first pile of pallets and the second heat flux meter (the first heat flux meter was positioned upstream of the first pile). The spread rates between the third and fourth heat flux meter showed diverging results, which is due to that no pile of pallets was positioned downstream of the fourth heat flux meter. The highest spread rates - between the third and fourth heat flux meter - were recorded in the cases where the last pile of pallets was positioned closest to the fourth heat flux meter. The overall average fire spread rate of the various experiments was found to be similar, corresponding to approximately 0.1 m/s in full scale. See figure 18 for fire spread rates of experiment #3, #8, #9 and #11.

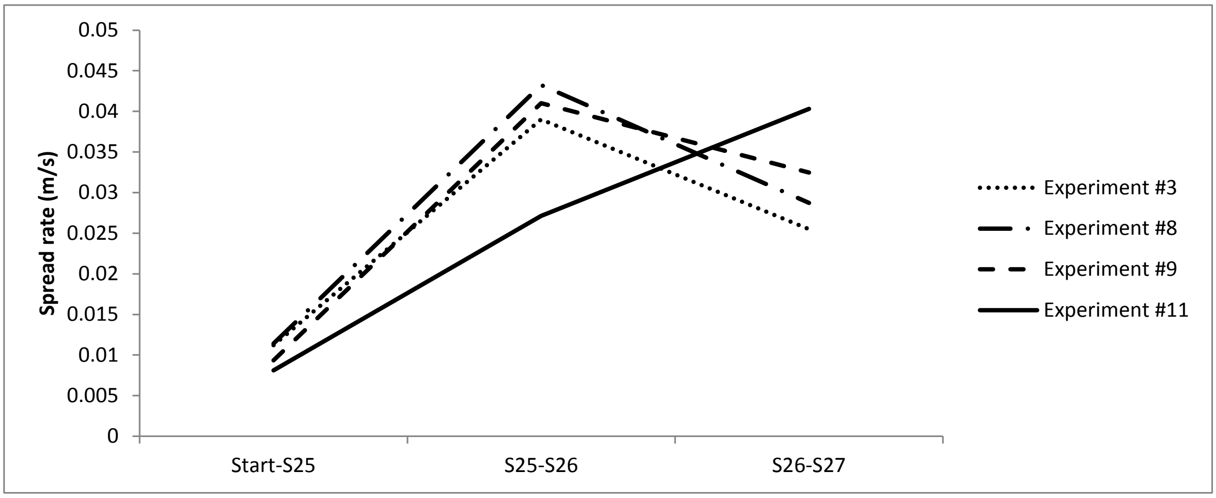

Figure 18. The fire spread rate between the different heat flux meters along the model scale mine drift/tunnel.

Similar results were obtained when applying the fire gas layer temperature criterion of 600°C at roof level to pinpoint the position of the fire at a given point of time. The fire accelerated considerably during parts of the distance, the fire spread rate increased approximately four times during the course. In figure 19, the fire spread rates between the different thermocouples at the roof level are displayed (starting with the distance between the first pile and thermocouple 6, see figure 4 for the position of the thermocouples) for experiments #4, #7, #8 and #9. As can be seen, the fire spread rate started to accelerate between thermocouple T8 (positioned in between the second and third pile) and T9 (positioned right after the third pile). The fire behaviour changed significantly after the second pile. Experiment #4 never underwent the acceleration phase as the other experiments, as experiment #4 was a reference experiment only containing one pile of wooden pallets. A spread rate of 0.1 m/s in the model scale experiments corresponds to a spread rate of approximately 0.4 m/s in full scale. After T9 and the acceleration phase the spread rates of the fires decreased and levelled out. Thermocouple T10 was positioned at or very close to the last pile of wooden pallets, the decreasing fire spread was due to that the fire lost momentum when it ran out of fuel.

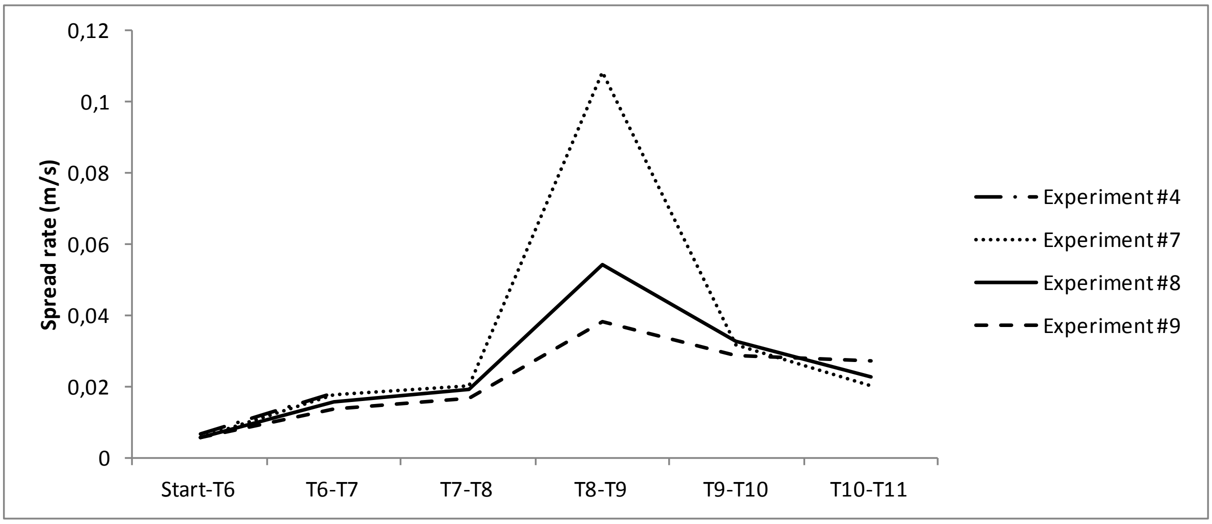

Figure 19. The fire spread rate between different thermocouples along the model scale mine drift/tunnel.

4.5 The heat release rates

The fire experiments were found to be fuel controlled applying equation (1) and the measured maximum heat release rates found in table 1 - and not ventilation controlled - throughout the entire duration of the fires. This is in line with the environment of a mine drift, where the longitudinal ventilation flow together with the large air masses available, making ventilation controlled fires less likely compared with for example compartment fires [2].

The dimensions of the model scale mine drift correspond to a height of 6 m and a width of 9 m in full scale. With a longitudinal ventilation velocity of 2.32 m/s (the full scale velocity corresponding to the model scale velocity of 0.6 m/s) the maximum heat release rate would be approximately 450 MW, which is a very large fire and not very likely in a mine drift.

After the ignition of the second pile of wooden pallets, flames started to tilt horizontally and fill up the entire cross section. See table 1 for the time points where the flames became horizontal and the corresponding heat release rates. If applying the heat release rate at the time of when the flames started to display this behaviour as a threshold for the severe fire behaviour, an average heat release rate of 240 kW (standard deviation of 40 kW) was calculated for the experiments. The equivalent full scale heat release rate would be approximately 209 MW.

Potential sites for such a high heat release rate could be places where larger vehicles are accumulated: a parking drift with larger vehicles parked side by side or a workshop servicing a number of larger vehicles.

5. Conclusions

The fire behaviour involving multiple fuel items in a mine drift with longitudinal ventilation was analysed. Focusing on the phenomena occurring during the fire spread between multiple items in a mine drift. It was found – based upon performed fire experiments in a model-scale mine drift – that:

> Even though a flashover in an open mine drift is less likely compared with an enclosure fire, a progressively advancing flashover in a mine drift with a spatial continuity of combustible items is a possibility and a risk.

> A fire involving multiple fuel items may lead to high fire gas temperatures and flames across the entire cross section of the mine drift and with flames tilted horizontally. Causing earlier ignition, higher fire growth rate, higher maximum heat release rate, increasing fire spread rate and more severe fire behaviour.

> A fire scenario in a mine drift where fuel surfaces in the lower regions are exposed to a larger degree of convection, flame radiation and flame impingement may have a severe impact on the fire safety. Larger amount of combustible materials are found in the lower regions and fire protection systems may not have been designed with respect to the severe fire behaviour.

> The measured flame lengths showed increasing and longer flame lengths with each ignited fuel item further downstream, due to decreasing air entrainment. A correlation for the continuous flame length was analysed and proposed for multiple fires in a mine drift.

> The analysis further underlines the importance of preventing the fire from spreading to an adjacent, larger fuel item. Preventing a severe and accelerating fire behaviour that could have disastrous effects in an underground mine.

The findings of the analysis would help identifying and preventing potentially dangerous fire situations and improve the design of fire safety measures with respect to the fire behaviour.

6. References

[1] Hansen R, Ingason H. Heat Release Rates of Multiple Objects at Varying Distances. Fire Safety Journal 2012;52:1-10.

[2] Hansen R. Study of heat release rates of mining vehicles in underground hard rock mines. Doctoral thesis. Västerås: Mälardalen University; 2015.

[3] Thomas PH, Baldwin R, Heselden JM. Buoyant Diffusion Flames: Some Measurements of Air Entrainment, Heat Transfer, and Flame Merging. Tenth International Symposium on Combustion 1965;983-996.

[4] Baldwin R. Flame Merging in Multiple Fires. Combustion and Flame 1968;12:318-324.

[5] Kamikawa D, Weng WG, Kagiya K, Fukuda Y, Mase R, Hasemi Y. Experimental study of merged flames from multifire sources in propane and wood crib burners. Combustion and Flame 2005;142:17-23.

[6] Wan H, Gao Z, Ji J, Li K, Sun J, Zhang Y. Experimental study on ceiling gas temperature and flame performances of two buoyancy-controlled propane burners located in a tunnel. Applied Energy 2017;185:573-581.

[7] Ji J, Wan H, Gao Z, Fu Y, Sun J, Zhang Y, Li K, Hostikka S. Experimental study on flame merging behaviors from two pool fires along the longitudinal centerline of model tunnel with natural ventilation. Combustion and Flame 2016;173:307-318.

[8] Ingason H. Model Scale Tunnel Fire Tests, SP report 2005:49. Borås: Swedish National Testing and Research Institute; 2005.

[9] Hansen R, Ingason H. An engineering tool to calculate heat release rates of multiple objects in underground structures. Fire Safety Journal 2011;46:194-203.

[10] De Rosa MI. Analysis of mine fires for all US metal/non-metal mining categories, 1990–2001. NIOSH; 2004.

[11] Hansen R. Investigation on fire causes and fire behaviour – vehicle fires in underground mines in Sweden 1988–2010. Work report SiST 2013:3. Västerås: Mälardalen University; 2013.

[12] Beard A, Carvel R. The handbook of tunnel fire safety. London: Thomas Telford Ltd; 2005.

[13] Li YZ, Ingason H. Maximum ceiling temperature in a tunnel fire. SP Report 2010:51, Borås: SP Swedish National Testing and Research Institute; 2010.

[14] Ingason H, Li YZ. Model scale tunnel fire tests with longitudinal ventilation. Fire Safety Journal 2010;45:371–384.

[15] Hansen R. Analysis of Methodologies for Calculating the Heat Release Rates of Mining Vehicle Fires in Underground Mines. Fire Safety Journal 2015;71:194–216.

[16] Hansen R, Ingason H. Model scale fire experiments in a model tunnel with wooden pallets at varying distances. Research report SiST 2010:8. Västerås: Mälardalen University; 2010.

[17] Quintiere JG. Fundamentals of fire phenomena. Chichester: John Wiley & Sons Ltd; 2006.

[18] Heskestad G. Fire Plumes, Flame Height and Air Entrainment. In: The SFPE Handbook of Fire Protection Engineering, Ed: DiNenno PJ, NFPA, Quincy, USA; 2008.

[19] Quintiere JG. Scaling applications in fire research. Fire Safety Journal 1989;15:3-29.

[20] Zukoski EE. Properties of fire plumes, Combustion fundamentals of fire. London: Academic Press; 1995.